doi:10.6041/j.issn.1000-1298.2014.04.051

双曲面加工干涉区域分析*

黄志东[1,2]　张　雷[1]　赵　继[1]

(1.吉林大学机械科学与工程学院,长春 130025;2.辽宁科技学院机械工程学院,本溪 117004)

摘要:针对复杂曲面中较为常见的双曲面进行了研究,建立了加工双曲面的数学模型,通过对双曲面参数特征的分析,发现了双曲面上任意点的切线斜率极限值以及刀具轴线斜率极限值的变化规律,据此推导出双曲面参数、刀具参数与偏心率平方之间的函数关系,推演了加工双曲面不发生干涉的参数准则,同时明确了切削角与偏心率平方满足不同函数关系对应的干涉区域。通过仿真实验,验证了理论分析的正确性,为加工双曲面的参数选取提供依据。

关键词:双曲面　加工　干涉　分析

中图分类号:TG659　　**文献标识码**:A　　**文章编号**:1000-1298(2014)04-0322-05

引言

以叶片和光学非球面透镜为代表的复杂曲面零件的应用越来越广泛,加工技术越来越受到各国学者的重视[1-3]。在现代高推重比航空发动机结构中,采用整体叶盘结构避免了榫头气流损失,减少了零件质量和零件数,使得发动机的推重比和可靠性得到了进一步的提高[4]。在光学系统中,采用非球面透镜可以校正像差,提高光学系统成像质量,并且多个球面零件可由一个或几个非球面零件代替,以达到简化仪器结构,降低成本和减轻仪器质量的目的[5]。文献[6-7]研究了叶片加工干涉检验与无干涉刀位轨迹规划算法。文献[8]解决了非球面加工的 NURBS 建模。比较成熟的非球面加工方法有平行磨削法[9-11]、圆弧包络磨削法[12]、双圆弧插补法[13-14]以及慢刀伺服[15]等。文献[16]设计了六轴高精密机床并将其应用于非球面光学镜面的加工。而对非球面的测量方法主要有干涉法、坐标测量法、激光扫描法[17]。文献[18]实现了大型光学非球面的测量。文献[19]通过在线检测完成误差补偿。然而,无论加工还是检测,工具与复杂曲面之间的干涉问题不容忽视。本文针对复杂曲面中较为常见的双曲面进行研究,建立加工双曲面的数学模型,分析加工双曲面的参数特征,推导加工双曲面不发生干涉的参数准则,并进行仿真实验。

1　加工双曲面的数学模型

二次曲面的子午截面曲线[20]可表示为

$$y^2 = 2\rho z - (1 - e^2)z^2 \tag{1}$$

式中　ρ——曲线顶点的曲率半径

e——曲线的偏心率

z——曲线的纵坐标

当 $e^2 > 1$ 时,二次曲面为双曲面。在加工双曲面时,可以只研究 $z \geqslant 0$ 的部分,故其子午截面曲线的函数表达式为

$$z = \frac{\rho}{1 - e^2} + \sqrt{\left(\frac{\rho}{1 - e^2}\right)^2 - \frac{y^2}{1 - e^2}} \tag{2}$$

加工双曲面的数学模型如图 1 所示,以双曲线的顶点 O_1 为原点,水平向右为 Y 轴正方向,竖直向上为 Z 轴正方向,建立直角坐标系。对双曲线上任意一点 $O_2(y_2, z_2)$,存在一条过点 O_2 且与双曲线相切的直线 l_0,其斜率为 k_0。直线 l_2 为刀具轴线,O_3 为刀头回转中心,连接 O_2O_3,作直线 l_1。直线 l_1 与直线 l_2 的夹角为 α。不同的 α 对应不同的刀具切削点位置,为了提高表面质量,在整个加工过程中,必须保持刀具切削点位置不变,即 α 保持不变,称 α 为切削角。

2　加工双曲面的参数

2.1　双曲面参数 k_0

双曲线上任意点 O_2 的切线 l_0 的斜率 k_0 为

收稿日期:2013-05-11　修回日期:2013-06-08

*国家高技术研究发展计划(863 计划)资助项目(2012AA041304)、国家重点基础研究发展计划(973 计划)资助项目(2011CB706702)和吉林大学研究生创新基金资助项目(20121078)

作者简介:黄志东,博士生,辽宁科技学院讲师,主要从事智能精密制造研究,E-mail:hzdstarcraft@126.com

通讯作者:张雷,教授,博士生导师,主要从事智能精密制造研究,E-mail:zhanglei@jlu.edu.cn

$$k_0 = \frac{y_2}{\rho - (1 - e^2) z_2} \tag{3}$$

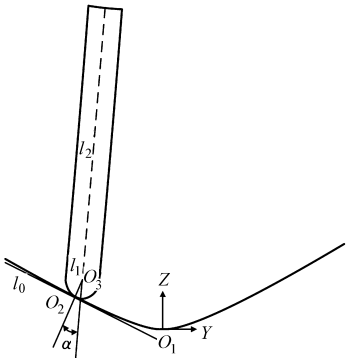

图 1　加工双曲面的数学模型

Fig. 1　Mathematical model for machining hyperboloidal surface

根据式(2)可知

$$z_2 = \frac{\rho}{1 - e^2} + \sqrt{\left(\frac{\rho}{1 - e^2}\right)^2 - \frac{y_2^2}{1 - e^2}} \tag{4}$$

将式(4)代入式(3),可得

$$k_0 = \frac{y_2}{\sqrt{\rho^2 + y_2^2 (e^2 - 1)}} \tag{5}$$

当 e^2 取不同值时,$k_0 - y_2$ 曲线如图 2 所示。

由式(5)可推出

$$\begin{cases} k_{0\min} = \lim\limits_{y_2 \to -\infty} k_0 = \lim\limits_{y_2 \to -\infty} \dfrac{y_2}{\sqrt{\rho^2 + y_2^2 (e^2 - 1)}} = -\dfrac{1}{\sqrt{e^2 - 1}} \\ k_{0\max} = \lim\limits_{y_2 \to +\infty} k_0 = \lim\limits_{y_2 \to +\infty} \dfrac{y_2}{\sqrt{\rho^2 + y_2^2 (e^2 - 1)}} = \dfrac{1}{\sqrt{e^2 - 1}} \end{cases} \tag{6}$$

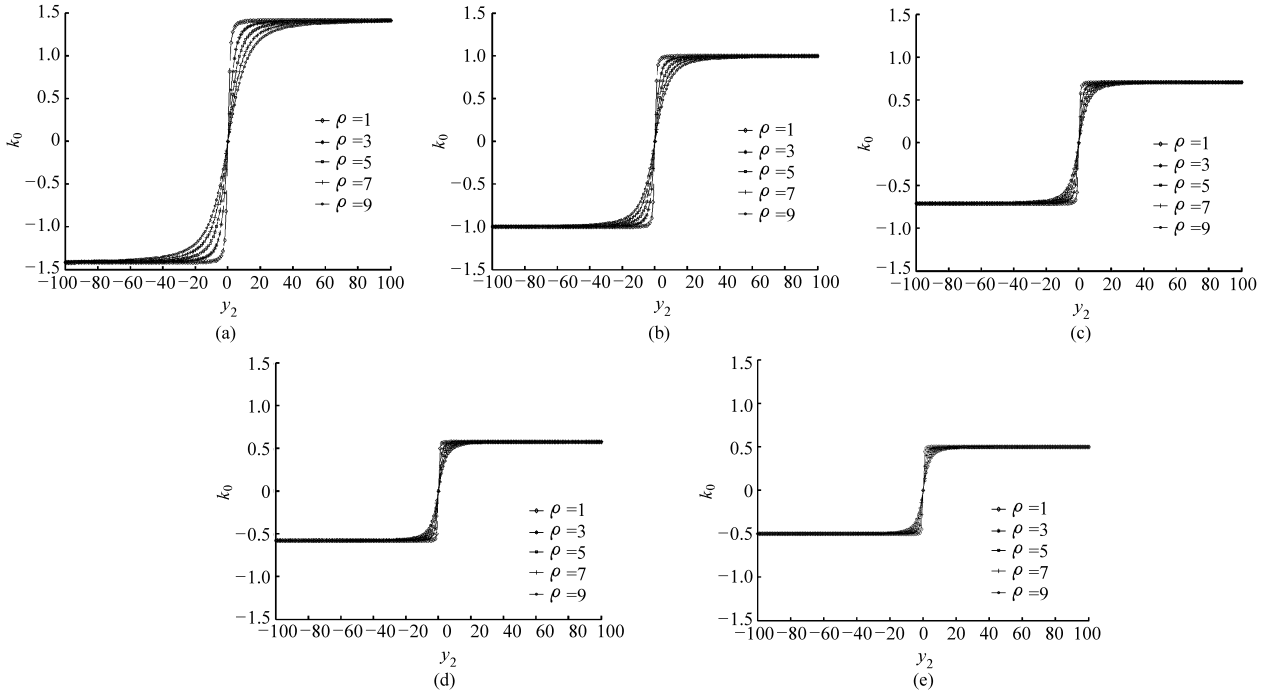

图 2　$k_0 - y_2$ 曲线

Fig. 2　The $k_0 - y_2$ curve

(a) e^2 =1.5　(b) e^2 =2　(c) e^2 =3　(d) e^2 =4　(e) e^2 =5

由式(6)可知,当 y_2 趋于无穷大时,k_0 的极限值只与 e^2 有关,而与 ρ 无关。k_0 的极限值随 e^2 的变化曲线如图 3 所示。

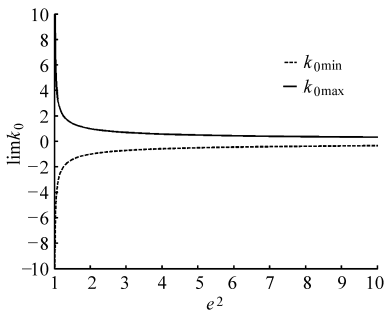

图 3　$\lim k_0 - e^2$ 曲线

Fig. 3　The $\lim k_0 - e^2$ curve

2.2　刀具参数 k_1 和 k_2

直线 l_1 的斜率 k_1 为

$$k_1 = -\frac{1}{k_0} \tag{7}$$

以 e^2 =3、ρ =2 的双曲线为例,其 $k_1 - y_2$ 曲线如图 4 所示。

由式(6)和式(7)可推出

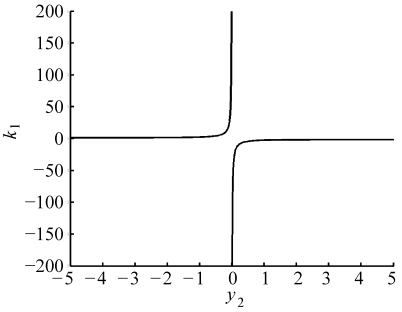

图 4 $k_1 - y_2$曲线

Fig. 4 The $k_1 - y_2$ curve

$$\begin{cases} \lim\limits_{y_2 \to -\infty} k_1 = \sqrt{e^2 - 1} \\ k_1(y_2 = 0) = +\infty \\ \lim\limits_{y_2 \to +\infty} k_1 = -\sqrt{e^2 - 1} \end{cases} \tag{8}$$

因此 k_1 的取值范围为 $k_1 > \sqrt{e^2 - 1}$ 或 $k_1 < -\sqrt{e^2 - 1}$。k_1的取值范围随 e^2的变化曲线如图 5 所示。

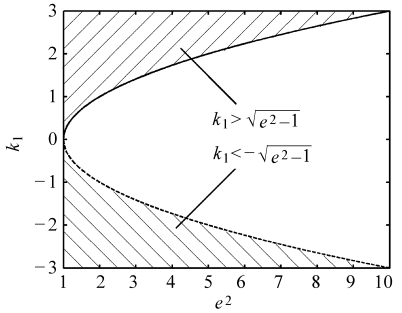

图 5 $k_1 - e^2$曲线

Fig. 5 The $k_1 - e^2$ curve

根据图 1 中 l_1与 l_2的几何关系,可知 α 与 k_1、k_2 的关系为

$$\tan\alpha = \frac{k_2 - k_1}{1 + k_1 k_2} \tag{9}$$

由式(9)可推出

$$k_2 = \frac{k_1 + \tan\alpha}{1 - k_1 \tan\alpha} \tag{10}$$

由于轴对称非球面具有对称性,因此这里只需讨论切削点 $y \leqslant 0$ 的部分。在这个区域里,k_1始终为“+”,而 $\tan\alpha$ 也为“+”。

于是,由式(10)可知

$$\begin{cases} k_2 > 0 & (k_1 \tan\alpha < 1) \\ k_2 < 0 & (k_1 \tan\alpha > 1) \end{cases} \tag{11}$$

$k_2 > 0$ 时存在最小值 $k_{2\min}$;$k_2 < 0$ 存在最大值 $k_{2\max}$。

由式(8)和式(10)可推出

$$\begin{cases} k_{2\min} = \lim\limits_{y_2 \to -\infty} k_2 = \lim\limits_{y_2 \to -\infty} \dfrac{k_1 + \tan\alpha}{1 - k_1 \tan\alpha} = \\ \qquad \dfrac{\lim\limits_{y_2 \to -\infty} k_1 + \tan\alpha}{1 - \lim\limits_{y_2 \to -\infty} k_1 \tan\alpha} = \dfrac{\sqrt{e^2 - 1} + \tan\alpha}{1 - \sqrt{e^2 - 1}\tan\alpha} \\ k_{2\max} = \lim\limits_{y_2 \to 0} k_2 = \lim\limits_{y_2 \to 0} \dfrac{k_1 + \tan\alpha}{1 - k_1 \tan\alpha} = \\ \qquad \lim\limits_{y_2 \to 0} \dfrac{1 + \dfrac{\tan\alpha}{k_1}}{\dfrac{1}{k_1} - \tan\alpha} = \dfrac{1 + \lim\limits_{y_2 \to 0} \dfrac{\tan\alpha}{k_1}}{\lim\limits_{y_2 \to 0} \dfrac{1}{k_1} - \tan\alpha} = -\dfrac{1}{\tan\alpha} \end{cases} \tag{12}$$

3 加工双曲面不发生干涉的参数准则

当满足条件

$$\begin{cases} \Delta_1 = k_{2\min} - k_{0\max} > 0 \\ \Delta_2 = k_{2\max} - k_{0\min} < 0 \end{cases} \tag{13}$$

刀具与工件将不存在干涉。

3.1 条件 1

将式(6)和式(12)代入式(13),可得

$$\Delta_1 = \frac{\sqrt{e^2 - 1} + \tan\alpha}{1 - \sqrt{e^2 - 1}\tan\alpha} - \frac{1}{\sqrt{e^2 - 1}} = \frac{e^2 - 2 + 2\sqrt{e^2 - 1}\tan\alpha}{\sqrt{e^2 - 1}(1 - \sqrt{e^2 - 1}\tan\alpha)} > 0 \tag{14}$$

由于 $k_1 > \sqrt{e^2 - 1}$ 且 $k_2 > 0$,由式(11)可得 $\sqrt{e^2 - 1}\tan\alpha < k_1 \tan\alpha < 1$,即式(14)中的分母

$$\sqrt{e^2 - 1}(1 - \sqrt{e^2 - 1}\tan\alpha) > 0 \tag{15}$$

于是分子也应大于零,即

$$e^2 - 2 + 2\sqrt{e^2 - 1}\tan\alpha > 0 \tag{16}$$

可解得

$$\alpha > \arctan\frac{2 - e^2}{2\sqrt{e^2 - 1}} \tag{17}$$

3.2 条件 2

将式(6)和式(12)代入式(13),可得

$$\Delta_2 = -\frac{1}{\tan\alpha} - \left(-\frac{1}{\sqrt{e^2 - 1}}\right) < 0 \tag{18}$$

可解得

$$\alpha < \arctan\sqrt{e^2 - 1} \tag{19}$$

3.3 参数分析

根据条件 1 和条件 2 可知,当同时满足式(17)和式(19)时,即 α 与 e^2的函数关系满足图 6 中第 1 区域,工具与双曲面不会出现干涉现象。图 6 中的第 2 区域表示工具与双曲面右侧会出现干涉现象;第 3 区域表示工具与双曲面左右两侧均会出现干涉现象;第 4 区域则表示工具与双曲面左侧会出现干涉现象。

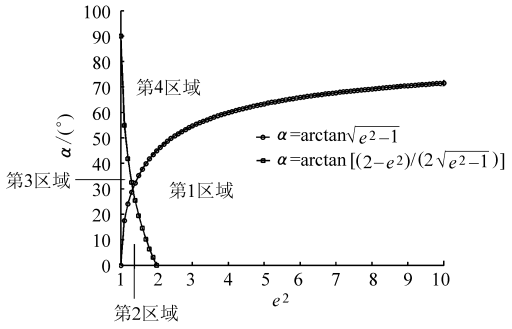

图 6　$\alpha - e^2$ 曲线

Fig. 6　The $\alpha - e^2$ curve

4　仿真实验

4.1　仿真实验 1

实验参数设定：双曲面参数 $e^2 = 4, \rho = 3$，刀具参数 $r = 1, \alpha = 20°$。由图 6 可知，α 与 e^2 的函数关系位于第 1 区域。仿真实验如图 7 所示。由图 7 可得刀具与工件不会发生干涉碰撞。

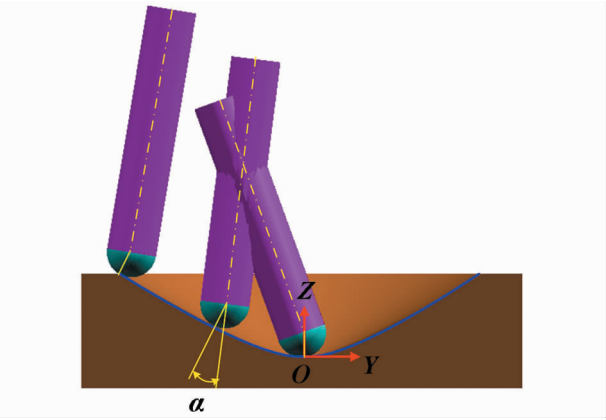

图 7　仿真实验 1

Fig. 7　The first simulation experiment

4.2　仿真实验 2

实验参数设定：双曲面参数 $e^2 = 1.5, \rho = 3$，刀具参数 $r = 1, \alpha = 5°$。由图 6 可知，α 与 e^2 的函数关系位于第 2 区域。仿真实验如图 8 所示。由图 8 可得刀具与工件在右侧发生干涉碰撞。

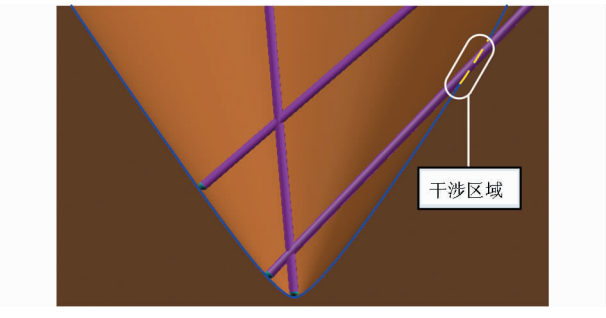

图 8　仿真实验 2

Fig. 8　The second simulation experiment

4.3　仿真实验 3

实验参数设定：双曲面参数 $e^2 = 1.2, \rho = 3$，刀具参数 $r = 1, \alpha = 25°$。由图 6 可知，α 与 e^2 的函数关系位于第 3 区域。仿真实验如图 9 所示。由图 9 可得刀具与工件在左右两侧均发生干涉碰撞。

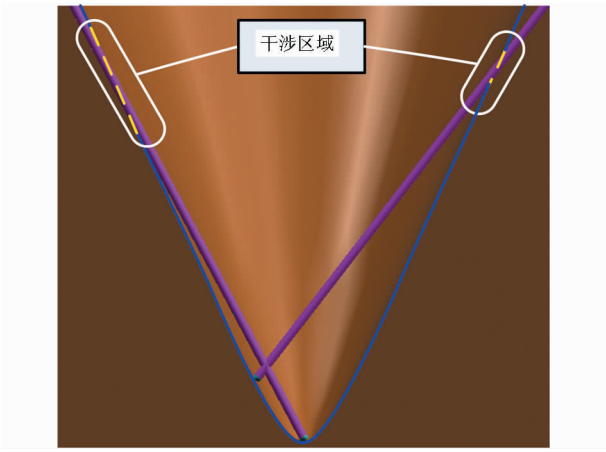

图 9　仿真实验 3

Fig. 9　The third simulation experiment

4.4　仿真实验 4

实验参数设定：双曲面参数 $e^2 = 1.33, \rho = 3$，刀具参数 $r = 1, \alpha = 40°$。由图 6 可知，α 与 e^2 的函数关系位于第 4 区域。仿真实验如图 10 所示。由图 10 可得刀具与工件在左侧发生干涉碰撞。

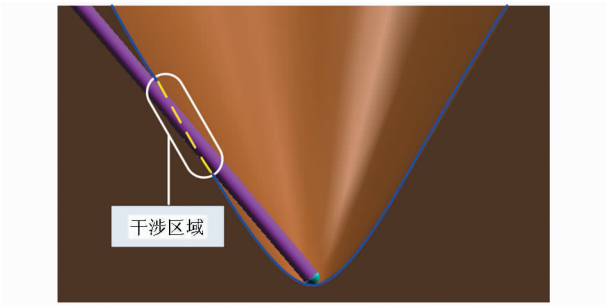

图 10　仿真实验 4

Fig. 10　The fourth simulation experiment

5　结论

（1）建立了加工双曲面的数学模型，分析了加工双曲面的参数特征。推导了双曲面参数 k_0、刀具参数 k_1、k_2 与偏心率平方 e^2 之间的函数关系。

（2）推演了加工双曲面不发生干涉的参数准则，同时确定了工具与工件不会发生干涉碰撞、与工件右侧发生干涉碰撞、与工件左右两侧均发生干涉碰撞以及与工件左侧发生干涉碰撞时切削角度 α 与偏心率平方 e^2 满足的不同函数关系。

（3）通过仿真实验，验证了理论分析的正确性，为加工双曲面时选择合理的参数，避免发生干涉碰撞提供了理论依据。

参 考 文 献

1 樊成,张雷,袁俊,等. 基于粗糙集和模糊聚类的复杂曲面零件可制造性评价[J]. 农业机械学报,2013,44(10):253 - 259.
Fan Cheng, Zhang Lei, Yuan Jun, et al. Manufacturability evaluation of complex surface parts based on rough set theory and fuzzy clustering[J]. Transactions of the Chinese Society for Agricultural Machinery, 2013,44(10):253 - 259. (in Chinese)

2 马骊溟,徐毅,李泽湘. 基于旋量理论的复杂曲面定位算法[J]. 农业机械学报,2007,38(11):129 - 132.
Ma Liming, Xu Yi, Li Zexiang. Freeform surface localization algorithm based on screw theory[J]. Transactions of the Chinese Society for Agricultural Machinery, 2007,38(11):129 - 132. (in Chinese)

3 周波,赵吉宾,刘伟军. 复杂曲面五轴数控加工刀轴矢量优化方法研究[J]. 机械工程学报,2013,49(7):184 - 192.
Zhou Bo, Zhao Jibin, Liu Weijun. Method study on optimization of tool axis vector for complex surface of 5-axis CNC[J]. Journal of Mechanical Engineering, 2013,49(7):184 - 192. (in Chinese)

4 刘自成,舒发龙,张为民. 整体叶盘叶片加工变形控制技术研究[J]. 航空制造技术,2011(9):88 - 90.
Liu Zicheng, Shu Falong, Zhang Weimin. Study on control of machining deformation of blisk blade[J]. Aeronautical Manufacturing Technology,2011(9):88 - 90. (in Chinese)

5 陈钦芳,徐昌杰. 轴对称非球面透镜光轴共轴度的测量研究[J]. 应用光学,2008,29(6):870 - 873.
Chen Qinfang, Xu Changjie. Coaxial measurement of axisymmetric aspheric lens[J]. Journal of Applied Optics,2008,29(6):870 - 873. (in Chinese)

6 钟诗胜,杨晓钧,王知行. 七轴并联机床加工汽轮机叶片技术及其工作空间干涉检查研究[J]. 组合机床与自动化加工技术,2005(6):62 - 64.
Zhong Shisheng, Yang Xiaojun, Wang Zhixing. Turbine blade machining technologies by 7-axis parallel kinematics machine and workspace interference check[J]. Modular Machine Tool & Automatic Manufacturing Technique,2005(6):62 - 64. (in Chinese)

7 杨方飞,阎楚良,林洪义. 五轴数控加工叶片无干涉刀位轨迹的计算[J]. 农业机械学报,2003,34(2):97 - 100.
Yang Fangfei, Yan Chuliang, Lin Hongyi. Trajectory computation of an interference-free cutter for five-axis NC machining of blades[J]. Transactions of The Chinese Society for Agricultural Machinery,2003,34(2):97 - 100. (in Chinese)

8 Park H. A solution for NURBS modeling in aspheric lens manufacture[J]. The International Journal of Advanced Manufacturing Technology, 2004,23(1 ~ 2): 1 - 10.

9 Saeki M, Kuriyagawa T, Lee J S, et al. Machining of aspherical opto-device utilizing parallel grinding method[C]// Proceedings of the ASPE Annual Meeting, 2001: 433 - 436.

10 Chen W K, Kuriyagawa T, Huang H, et al. Machining of micro aspherical mould inserts[J]. Precision Engineering, 2005, 29(3):315 - 323.

11 林晓辉,郭隐彪,王振忠,等. 大尺寸轴对称非球面磨削精度建模和分析[J]. 机械工程学报,2013,49(17):65 - 72.
Lin Xiaohui, Guo Yinbiao, Wang Zhenzhong, et al. Precision model and analysis of large axisymmetric aspheric grinding[J]. Journal of Mechanical Engineering, 2013,49(17):65 - 72. (in Chinese)

12 Kuriyagawa T, Zahmaty M S S, Syoji K. A new grinding method for aspheric ceramic mirrors[J]. Journal of Materials Processing Technology, 1996,62(4): 387 - 392.

13 Lee T M, Lee E K, Yang M Y. Precise bi-arc curve fitting algorithm for machining an aspheric surface[J]. The International Journal of Advanced Manufacturing Technology, 2007,31(11 ~ 12): 1191 - 1197.

14 张学忱,陈锦昌,申艺杰. 基于周对称非球面子午线的步长不变式双圆弧插补算法[J]. 机械工程学报,2013,49(9):144 - 150.
Zhang Xuechen, Chen Jinchang, Shen Yijie. The step constant double circular interpolation algorithm research based on axisymmetric aspheric meridian[J]. Journal of Mechanical Engineering, 2013,49(9):144 - 150. (in Chinese)

15 Yin Z Q, Dai Y F, Li S Y, et al. Fabrication of off-axis aspheric surfaces using a slow tool servo[J]. International Journal of Machine Tools and Manufacture, 2011,51(5): 404 - 410.

16 Cheng H B, Feng Z J, Cheng K, et al. Design of a six-axis high precision machine tool and its application in machining aspherical optical mirrors[J]. International Journal of Machine Tools & Manufacture, 2005,45(9): 1085 - 1094.

17 Ye Junjun, Guo Jiang, Guo Yinbiao. Research on path planning and data processing system for high-precise aspheric measurement[C]// Proceedings of SPIE, 2007,6723: 67235R-1 - 67235R-6.

18 Xiao M, Jujo S, Takahashi S, et al. Nanometer profile measurement of large aspheric optical surface by scanning deflectometry with rotatable devices: uncertainty propagation analysis and experiments[J]. Precision Engineering, 2012,36(1): 91 - 96.

19 Chen F J, Yin S H, Huang H, et al. Profile error compensation in ultra-precision grinding of aspheric surfaces with on-machine measurement[J]. International Journal of Machine Tools and Manufacture, 2010,50(5): 480 - 486.

20 潘君骅. 光学非球面的设计、加工与检验[M]. 苏州:苏州大学出版社, 2004: 1 - 9.

(下转第 321 页)

spheres[C]// Proceedings of the IEEE International Conference on Image Processing, 2003:757 - 760.
11 Engineering Shape Benchmark. http://shapelab.ecn.purdue.edu.
12 Jayanti S, Kalyanaraman Y, Iyer N, et al. Developing an engineering shape benchmark for CAD models [J]. Computer-Aided Design, 2006, 38(9): 939 - 953.
13 Patel N V, Sethi I K. Video shot detection and characterization for video databases [J]. Pattern Recognition, 1997, 30(4):583 - 592.
14 Hong T, Lee K, Kim S, et al. Similarity comparison of mechanical parts [J]. Computer-Aided Design & Applications, 2005, 2(6): 759 - 768.
15 Hong T, Lee K, Kim S. Similarity comparison of mechanical parts to reuse existing designs [J]. Computer-Aided Design, 2006, 38(9): 973 - 984.

3-D CAD Model Retrieval Algorithm Based on Distance and Angle Distributions

Zhang Kaixing[1]　Huang Rui[2]　Liu Xianxi[3]
(1. *College of Mechanical and Electronic Engineering*, *Shandong Agricultural University*, *Taian* 271018, *China*
2. *School of Mechanical Engineering*, *Northwestern Polytechnical University*, *Xi'an* 710072, *China*
3. *Shandong Provincial Key Laboratory of Horticultural Machineries and Equipments*, *Shandong Agricultural University*, *Taian* 271018, *China*)

Abstract: To reuse 3-D CAD models more efficiently, a 3-D CAD model retrieval algorithm based on distance and angle distributions was proposed. Firstly, a large number of random points on the model surface were taken to calculate the length of the directed line constructed between two random points and the angle between the normal of the point and the directed line. Then, a distance - angle planar grid was constructed to express the distance - angle distribution by obtaining a statistic data of the sampled points. At last, the Manhattan distance metric method was used to compute the similarity between the two distance - angle matrices, which can give the similarity coefficient for two compared 3-D CAD models. Experiments results show that the algorithm can effectively support 3-D CAD model retrieval, and the efficiency meets the requirements of engineering application.

Key words: 3-D model retrieval　Reusable　Shape distributions　Distance - angle distributions

(上接第 326 页)

Analysis of Interference Area in Machining Hyperboloidal Surface

Huang Zhidong[1,2]　Zhang Lei[1]　Zhao Ji[1]
(1. *College of Mechanical Science and Engineering*, *Jilin University*, *Changchun* 130025, *China*
2. *Department of Mechanical Engineering*, *Liaoning Institute of Science and Technology*, *Benxi* 117004, *China*)

Abstract: The hyperboloidal surface was studied, which was common in complex surfaces. The mathematical model for machining hyperboloidal surface was set up. Based on the analysis of parameter characteristics of hyperboloidal surface, the variation law of the slope limit value of tangent at arbitrary point on hyperboloidal surface and the slope limit value of the axis of tool was discovered. Based on the variation law, the functional relationship between parabola parameter, tool parameter and the square of eccentricity was obtained. The parameter criterion, by which the interference on machining hyperboloidal surface could be avoided, was deduced. The interference areas corresponding to different functional relationships between cutting angle and the square of eccentricity were clarified. The simulation experiment results showed the validity of theoretical analysis, which facilitated the parameter selection for machining hyperboloidal surface.

Key words: Hyperboloidal surface　Machining　Interfecrence　Analysis